The ISME Journal (2015) 9, 1062–1075

www.nature.com/ismej

OPEN

ORIGINAL ARTICLE

Differential contributions of ammonia oxidizers and nitrite oxidizers to nitrification in four paddy soils

Baozhan Wang[1,3], Jun Zhao[1,2,3], Zhiying Guo[1,2], Jing Ma[1], Hua Xu[1] and Zhongjun Jia[1]
[1]*State Key Laboratory of Soil and Sustainable Agriculture, Institute of Soil Science, Chinese Academy of Sciences, Nanjing, Jiangsu Province, People's Republic of China and* [2]*University of Chinese Academy of Sciences, Beijing, People's Republic of China*

Rice paddy fields are characterized by regular flooding and nitrogen fertilization, but the functional importance of aerobic ammonia oxidizers and nitrite oxidizers under unique agricultural management is poorly understood. In this study, we report the differential contributions of ammonia-oxidizing archaea (AOA), bacteria (AOB) and nitrite-oxidizing bacteria (NOB) to nitrification in four paddy soils from different geographic regions (Zi-Yang (ZY), Jiang-Du (JD), Lei-Zhou (LZ) and Jia-Xing (JX)) that are representative of the rice ecosystems in China. In urea-amended microcosms, nitrification activity varied greatly with 11.9, 9.46, 3.03 and 1.43 μg NO_3^--N g^{-1} dry weight of soil per day in the ZY, JD, LZ and JX soils, respectively, over the course of a 56-day incubation period. Real-time quantitative PCR of *amoA* genes and pyrosequencing of 16S rRNA genes revealed significant increases in the AOA population to various extents, suggesting that their relative contributions to ammonia oxidation activity decreased from ZY to JD to LZ. The opposite trend was observed for AOB, and the JX soil stimulated only the AOB populations. DNA-based stable-isotope probing further demonstrated that active AOA numerically outcompeted their bacterial counterparts by 37.0-, 10.5- and 1.91-fold in ^{13}C-DNA from ZY, JD and LZ soils, respectively, whereas AOB, but not AOA, were labeled in the JX soil during active nitrification. NOB were labeled to a much greater extent than AOA and AOB, and the addition of acetylene completely abolished the assimilation of $^{13}CO_2$ by nitrifying populations. Phylogenetic analysis suggested that archaeal ammonia oxidation was predominantly catalyzed by soil fosmid 29i4-related AOA within the soil group 1.1b lineage. *Nitrosospira* cluster 3-like AOB performed most bacterial ammonia oxidation in the ZY, LZ and JX soils, whereas the majority of the ^{13}C-AOB in the JD soil was affiliated with the *Nitrosomona communis* lineage. The ^{13}C-NOB was overwhelmingly dominated by *Nitrospira* rather than *Nitrobacter*. A significant correlation was observed between the active AOA/AOB ratio and the soil oxidation capacity, implying a greater advantage of AOA over AOB under microaerophilic conditions. These results suggest the important roles of soil physiochemical properties in determining the activities of ammonia oxidizers and nitrite oxidizers.
The ISME Journal (2015) **9,** 1062–1075; doi:10.1038/ismej.2014.194; published online 10 October 2014

Introduction

Nitrification, the biological oxidation of ammonia to nitrate via nitrite, is a central component of the global nitrogen cycle (Galloway *et al.*, 2008). Synthetic nitrogen fertilizer input in China accounts for more than 37% of the global nitrogen consumption with ~1.2 million tons in 2012, which was mostly in the form of ammonium (Food and Agricultural Organization of the United Nations (FAO), 2014). These ammonium fertilizers must be oxidized at least once before it is returned as N_2 into the atmosphere. Agricultural runoffs thus often contained excessively high amount of nutrient nitrate generated from ammonia oxidation and resulted in severe environmental pollution such as groundwater contamination (Sebilo *et al.*, 2013). It is also widely accepted that agricultural ecosystem is an important source of greenhouse gas N_2O (Yan *et al.*, 2003), a by-product during microbial ammonia oxidation (Klotz and Stein, 2008; Santoro *et al.*, 2011; Stieglmeier *et al.*, 2014). Nitrification has thus received worldwide attentions in past decades (Koops *et al.*, 2006).

Aerobic ammonia oxidation is carried out by phylogenetically distinct groups of ammonia-oxidizing archaea (AOA) and bacteria (AOB) in the first and rate-limiting step of nitrification (Könneke *et al.*, 2005). Microbial ecology of AOA and AOB often necessitates the analysis of biomarker *amoA* gene encoding the active-site polypeptide of

Correspondence: Z Jia, State Key laboratory of Soil and Sustainable Agriculture, Institute of Soil Science, Chinese Academy of Sciences, East Beijing Road No. 71, Xuan-Wu District, Nanjing City, Jiangsu Province 210008, People's Republic of China.
E-mail: jia@issas.ac.cn
[3]These authors contributed equally to this work.
Received 11 June 2014; revised 19 August 2014; accepted 22 August 2014; published online 10 October 2014

ammonia monooxygenase (Rotthauwe *et al.*, 1997; Francis *et al.*, 2005; Dam *et al.*, 2014), although the underlying mechanisms of enzymatic ammonia oxidation has not been fully understood (Hyman and Arp, 1992; Liew *et al.*, 2014). Nitrite oxidizers have immense ecological significance as a principal source of nitrate that supports primary biological production on Earth (Gruber and Galloway, 2008); additionally, these oxidizers have environmental importance for wastewater treatment (Lücker *et al.*, 2010). The ecophysiological study of nitrite-oxidizing bacteria (NOB), however, has long been hampered by the lack of specific assays to assess highly diverse NOB communities in complex environments (Freitag *et al.*, 2006; Sorokin *et al.*, 2012). With the advent of high-throughput sequencing techniques, NOB have recently received increasing attention (Bock and Wagner, 2006; Xia *et al.*, 2011; Sorokin *et al.*, 2012).

Nitrifying populations use a very restricted substrate range, yet the coexistence of AOA, AOB and NOB populations has been demonstrated in a wide variety of environments. This implies that these microbial guilds might have developed distinctly different lifestyles for resource utilization. For example, there are significant differences in the ammonia oxidation activity of AOB within the *Nitrosospira* and *Nitrosomonas* genera (Webster *et al.*, 2005), and the ecological significance of AOB and AOA has been synthesized on the basis of their physiological diversity (Prosser and Nicol, 2012). A recent study has shown that AOA has by far the greatest substrate affinity identified for any autotrophic ammonia oxidizer, which is consistent with *in situ* nitrification kinetics measured in the low-nutrient open ocean (Martens-Habbena *et al.*, 2009). The cultivation of the obligate acidophilic *Nitrosotalea devanaterra* provided further evidence for the extraordinary capability of AOA to thrive in low-pH soil (Lehtovirta-Morley *et al.*, 2011). In stark contrast, increasing lines of evidence have implied the predominance of bacterial ammonia oxidizers in environments with high ammonium levels (Jia and Conrad, 2009; Xia *et al.*, 2011). However, ecological generalizations of the AOA and AOB populations have resulted from experimental investigations in physicochemically contrasting environments (Prosser and Nicol, 2012) and may be constrained by the high levels of environmental heterogeneity, as no single factor can determine the function and adaption of nitrifying populations in complex natural settings.

Rice fields are a unique anthropogenic aquatic ecosystem. Flooding management depletes oxygen rapidly beneath the soil surface, where an oxygen gradient can be formed within a few millimeters of the thin surface soil because of the diffusion of atmospheric oxygen through the flooding water, and in the rhizosphere because of oxygen leakage from the rice roots (Liesack *et al.*, 2000). AOA and AOB may compete with each other for the limited oxygen supply from microaerobic niches in the paddy field. Molecular studies have suggested that AOA are better adapted to the suboxic/anoxic conditions of paddy soils, leading to a higher abundance of AOA versus AOB (Chen *et al.*, 2008; Herrmann *et al.*, 2009; Bannert *et al.*, 2011). Furthermore, flooding often leads to the accumulation of electron donors in the organic matter of the soil and sequential reduction of electron acceptors, such as nitrate and sulfate (Kimura, 2000). Such changes in the soil physiochemical properties may also have important roles in the resource utilization patterns of the AOA, AOB and NOB populations (Ke *et al.*, 2013). Nonetheless, the linear correlation between soil characteristics and community structures may not necessarily represent the functional importance of nitrifying populations in complex soil (Prosser and Nicol, 2012). Therefore, DNA-based stable-isotope probing (SIP) was used to link nitrification activity with the taxonomic identity of active microorganisms in four paddy soils from different geographic regions of southern China. We also aimed to correlate active nitrifying populations with soil properties to achieve a better understanding of environmental factors that are likely to have shaped the community structure of ammonia oxidizers and nitrite oxidizers in the paddy ecosystem.

Materials and methods

Description of the paddy field sites

The flow diagram of the key steps in this study was shown in Figure 1. Soil samples for microcosm incubation were collected from four paddy fields across southern China (Supplementary Figure S1). All sites are located in a subtropical monsoon climate and have been cultivated with rice for more than 100 years. All fields received annual fertilization of $\sim$250–350 kg N ha^{-1} during the rice growing season, and irrigation management of paddy field was described in Supplementary Methods. Bulk soil (the top 0–20 cm) was collected from each site immediately after rice harvesting, when the fields had been drained for about a week. Soil samples were transported on ice to the laboratory immediately after sampling and were then homogenized through a 2 mm sieve. A 200-g subsample of each soil sample was stored at $-20\,^{\circ}$C for the incubation of SIP microcosms and molecular analysis, and the remainder of the soil was air dried for physiochemical analysis.

Physicochemical properties of the soil

Soil properties were analyzed including pH, soil organic matter and total nitrogen (Table 1), and described in Supplementary Methods. Soil oxidation capacity (OXC) was calculated using the following equation (Zhang *et al.*, 2009): soil $\mathrm{OXC} = 5 \times [NO_3^-] + 2 \times [\mathrm{Mn(IV)}] + [\mathrm{Fe(III)}] + 8 \times [SO_4^{2-}]$.

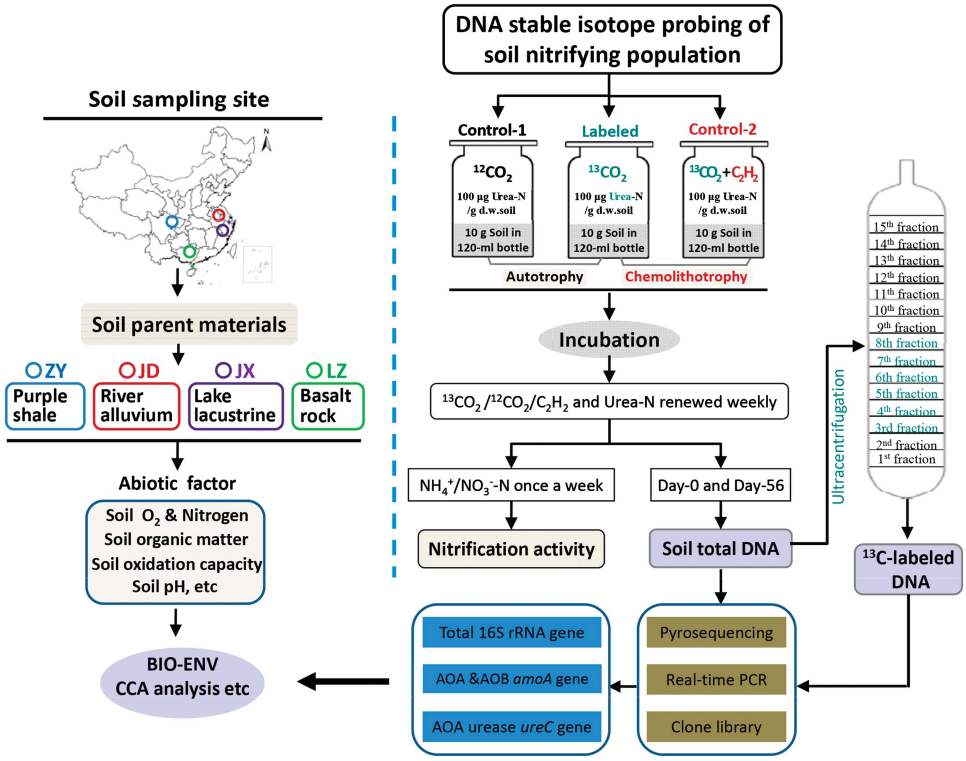

Figure 1 Flow diagram of the key experimental procedures in this study. The rice soils were collected from four paddy fields with different parent materials across southern China. The designations ZY, JD, LZ and JX represent rice fields from the cities of Zi-Yang, Jiang-Du, Lei-Zhou and Jia-Xing, respectively. DNA-SIP microcosms were constructed as described previously (Xia *et al.*, 2011). Three sets of DNA-SIP treatments were established including microcosms amended with $^{13}CO_2$, $^{12}CO_2$ and $^{13}CO_2 + C_2H_2$ (5% (vol vol^{-1}) CO_2, 100 Pa C_2H_2). A pairwise comparison between the $^{13}CO_2$-labeled and the $^{12}CO_2$ control treatment was used to assess whether the nitrifying populations assimilated $^{13}CO_2$ for autotrophic growth, and the $^{13}CO_2 + C_2H_2$ treatment was exploited to assess the chemolithotrophic dependence of $^{13}CO_2$ assimilation on ammonia oxidation that could be completely abolished by 100 Pa acetylene (Berg *et al.*, 1982). The headspace of the bottle was flushed once a week with pressurized synthetic air (20% O_2, 80% N_2), and the $^{13}CO_2$, $^{12}CO_2$ and C_2H_2 were renewed immediately after the headspace air exchange. Destructive sampling was performed in triplicate for extraction of soil total DNA and subsequent ultracentrifugation for molecular analysis. Soil physiochemical properties were also analyzed to investigate the relationship of active nitrifying populations to abiotic factors in the paddy ecosystem.

The soil OXC value represents the potential capacity of the soil to accept electrons because it includes all oxidizing agents in this equation; however, electron donors (such as soil organic matter) are not included. The brackets in the equation denote millimolar concentrations (mmol kg^{-1}). [Mn(IV)] and [Fe(III)] refer to the $NH_2OH \cdot HCl$-extractable Mn and Fe in free forms of soil iron oxides.

Microcosms of paddy soil were established in an attempt to mimic the redox status of the soil under *in situ* flooding conditions. Each 1500-ml polyethylene container (height, 30 cm; diameter, 8.0 cm) contained 1.5 kg of soil with 2–3 cm standing water, and the containers were kept static for 60 days at 25 °C. Vertical oxygen profiles were determined using an oxygen microelectrode sensor (Unisense OX 50; Science Park, Aarhus, Denmark). The microsensor tip was inserted into the soil in a stepwise manner for the measurement of soluble oxygen concentrations with an interval of 100 μm up to a final depth of 5 mm. The extended oxygen profile of the soil was then recorded at a 5-mm spatial resolution to a depth of 20 cm.

DNA-SIP microcosm and gradient fractionation

DNA-SIP microcosms were constructed as shown in Figure 1. All treatments were performed in triplicate microcosms and incubated at 60% of the soil maximum water-holding capacity at 28 °C in the dark. The $^{13}CO_2$ and $^{13}CO_2 + C_2H_2$ microcosms were amended with 100 μg ^{13}C-urea-N g^{-1} dry weight soil (d.w.s.), whereas the $^{12}CO_2$ treatments received 100 μg ^{12}C-urea-N g^{-1} d.w.s.on a weekly basis over the 8-week incubation period. Before incubation of SIP microcosms with carbon and ammonium substrates, the precondition was conducted as described in Supplementary Methods. The ^{13}C-urea and ^{12}C-urea (99 at% carbon) were purchased from the Shanghai Engineering Research Center of Stable Isotopes (Shanghai, China), and the$^{13}CO_2$ (99 at% carbon) was purchased from Sigma-Aldrich Co. (St Louis, MO, USA). $^{12}CO_2$ was produced by acidifying sodium carbonate. Destructive sampling was performed in triplicate for each treatment during the incubation period, and the soil samples were transferred immediately to a −80 °C freezer for subsequent molecular analysis. The remainder of

Table 1 Physiochemical properties of the paddy soils used in this study

Soil characteristics	*Zi-Yang*	*Jiang-Du*	*Lei-Zhou*	*Jia-Xing*
Location	N 30°05′ E 104°34′	N 32°35′ E 119°42′	N 20°33′ E 110°04′	N 30°38′ E 120°46′
MAT (°C)	16.8	14.9	22.0	15.9
MST of rice (°C)	25.6	27.0	26.2	25.8
MAR (mm)	965.8	978.7	1711.6	1168.6
pH	8.23	6.80	6.81	6.08
Total N ($g\,kg^{-1}$)	1.78	1.91	1.22	1.86
NO_3^--N ($mg\,kg^{-1}$)	6.84	7.25	1.35	11.35
NH_4^+-N ($mg\,kg^{-1}$)	17.58	4.62	8.01	33.94
SOM ($g\,kg^{-1}$)	30.4	35.4	10.2	12.0
Available P ($mg\,kg^{-1}$)	18.5	11.4	9.86	33.7
Available K ($mg\,kg^{-1}$)	104	62.5	184	137
OXC ($mmol\,kg^{-1}$)	7.40	9.21	19.94	27.27
NO_3^- N ($mg\,kg^{-1}$)	6.84	7.25	1.35	11.32
Mn (IV) ($mg\,kg^{-1}$)	2.65	4.37	10.20	84.37
Fe (III) ($mg\,kg^{-1}$)	31.9	19.5	30.5	43.5
SO_4^{2-} ($mg\,kg^{-1}$)	74.2	97.4	227.0	270.2
CEC ($cmol\,kg^{-1}$)	18.7	11.6	12.7	17.3
Particle size (%)				
Sand (50 μm–2 mm)	18.1	10.8	7.82	2.81
Silt (2–50 μm)	59.1	79.0	46.5	79.8
Clay (<2 μm)	22.8	10.2	45.7	17.4

Abbreviations: CEC, cation exchange capacity; MAR, mean annual rainfall; MAT, mean annual temperature; MST, mean seasonal temperature of rice cultivation; OXC, soil oxidation capacity; SOM, soil organic matter.

the soil sample was used for the determination of the inorganic nitrogen concentrations of NH_4^+-N, NO_2^--N and NO_3^--N in the soil. The detection limit was 0.01 mg $N\,l^{-1}$ for ammonium and 0.001 mg $N\,l^{-1}$ for nitrite and nitrate.

DNA was extracted from the soil samples using a FastDNA Spin Kit for Soil (MP Biomedicals, Cleveland, OH, USA), according to the manufacturer's instructions. Soil DNA quantity and purity were determined by a Nanodrop ND-1000 UV–vis Spectrophotometer (NanoDrop Technologies, Wilmington, DE, USA). SIP fractionation was performed as described previously (Xia *et al.*, 2011). For each treatment, ~3.0 μg of the DNA extract was mixed well with a CsCl stock solution to achieve an initial CsCl buoyant density of $1.725\,g\,ml^{-1}$.The isopycnic density centrifugation was performed using a 5.1 ml Quick-Seal polyallomer ultracentrifugation tube in a Vti65.2 vertical rotor (Beckman Coulter Inc., Palo Alto, CA, USA). The ^{13}C-labeled DNA was resolved from the native DNA by ultracentrifugation at 177 000 *g* for 44 h at 20 °C. DNA fractions were obtained by displacing the gradient medium with sterile water from the top of the ultracentrifuge tube using a syringe pump (New Era Pump Systems Inc., Farmingdale, NY, USA) with a precisely controlled flow rate of $0.38\,ml\,min^{-1}$. Approximately 14 or 15 DNA gradient fractions were generated with equal volumes of ~380 μl, and a 65 μl aliquot of each fraction was used for the refractive index measurement using an AR200 digital hand-held refractometer (Reichert Inc., Buffalo, NY, USA). The fractionated DNA was purified and dissolved in 30 μl of TE buffer as described previously (Freitag *et al.*, 2006).

Real-time PCR quantification of the amoA genes

Real-time quantitative PCR of the *amoA* genes was performed to determine the changes in abundances of AOA and AOB in the total DNA of the soil microcosms over an incubation period of 56 days. Additionally, the efficacy of ^{13}C incorporation into the genomes of AOA and AOB in the fractionated DNA across the entire buoyant density gradients from the DNA-SIP microcosms was also assessed by real-time PCR as described previously (Lu and Jia, 2013). The real-time PCR assay was conducted on a CFX96 Optical Real-Time Detection System (Bio-Rad Laboratories Inc., Hercules, CA, USA). The PCR conditions and primers are described in Supplementary Table S1. The real-time PCR standard was generated using plasmid DNA from one representative clone containing archaeal or bacterial *amoA* genes. A standard template dilution series from 5.48×10^1 to 5.48×10^8 copies per assay was used. A serial dilution of the DNA template was also used to assess whether the PCR was inhibited during the amplification. Real-time PCR was performed in biological triplicates with three technical replicates. Amplification efficiencies of 98–103% were obtained, with R^2 values of 0.997–0.999. A melting-curve and standard agarose gel electrophoresis was performed to check the specificity of the amplification products.

Pyrosequencing, cloning and phylogenetic analysis
Pyrosequencing of 16S rRNA genes in the V4 regions was conducted using the total DNA extract from soil microcosms amended with $^{13}CO_2$ and $^{13}CO_2 + C_2H_2$ at days 0 and 56 using a universal 515F–907R primer assay (Supplementary Table S2). In addition, the heavy DNA (fractions 3–8) obtained from isopycnic centrifugation of the total DNA extracts were also analyzed for the labeled (day 56—$^{13}CO_2$) and control (day 56—$^{12}CO_2$ and day 56—$^{13}CO_2 + C_2H_2$) microcosms (Supplementary Table S3) as described previously (Lu and Jia, 2013). Furthermore, pyrosequencing of archaeal and bacterial *amoA* genes in the total DNA extract was performed in soil microcosms amended with $^{13}CO_2$ at days 0 and 56 using the primers CrenamoA 23f/CrenamoA 616f (Tourna *et al.*, 2008) and *amoA*-1F/*amoA*-2R (Rotthauwe *et al.*, 1997), respectively (Supplementary Table S2). The fusion adapter A, followed by 6-nucleotide sample-specific barcode sequences, was added to the 5′ end of the forward primer, whereas adapter B was added to the 5′ end of the reverse primer. The PCR primers and thermal conditions are described in Supplementary Table S1. The PCR products were gel purified and further quantified using PicoGreen Kits (Invitrogen, Shanghai, China), and were pyrosequenced on a GS FLX Titanium sequencer (Roche Diagnostics Corporation, Branford, CT, USA).

The raw pyrosequencing data was processed using the PyroNoise algorithm within the mothur software package to remove sequence chimeras (Schloss *et al.*, 2009). The denoized sequence reads were then assigned to specific samples on the basis of unique barcode sequences, and only sequences >300 bp in length with an average quality score >30 and without ambiguous base calls were included in subsequent analyses. The taxonomic assignment for the major lineages of AOA, AOB and NOB was accomplished by binning the sequences of the 16S rRNA gene and the *amoA* gene into operational taxonomic unit (OTUs) at 97% similarity levels. A representative sequence within each OTU of the 16S rRNA or *amoA* gene was retrieved using the mothur software. All OTUs were taxonomically classified by the construction of neighbor-joining phylogenetic trees using representative sequences of the *amoA* and 16S rRNA genes. The taxonomy-determined reference sequences from the GenBank were included with the Kimura 2-parameter distance (determined using MEGA version 4.0), and 1000 replicates were used to generate the bootstrap values (Tamura *et al.*, 2007).

The archaeal and bacterial *amoA* genes in the ^{13}C-DNA were also amplified for clone library construction from the $^{13}CO_2$-labeled microcosm after incubation for 56 days, in addition to the *ureC* genes encoding the α-subunit of a putative archaeal urease (Lu and Jia, 2013). The PCR primers are described in Supplementary Table S1. The *Escherichia coli* JM109-competent cells were used for transformation. The sequencing of clones containing the correct insert was performed by the Invitrogen Sequencing Department (Invitrogen). A phylogenetic tree of the *amoA* genes was also constructed with MEGA version 4.0, as mentioned above.

Statistical analysis
BIO-ENV and canonical correspondence analysis (CCA) were used to identify abiotic factors likely to affect the microbial population of AOA and AOB in the four paddy soils under *in situ* conditions (Supplementary Table S5). The environmental variables were then used to construct a soil physicochemical property matrix for variation partitioning analysis in R within the vegan package. Spearman's correlation analysis was performed to assess the relationship between the soil properties and the AOA/AOB ratios in the^{13}C-DNA (Supplementary Table S6). A one-way analysis of variance was conducted, and Tukey's *post hoc* tests were performed for multiple comparisons. An independent-sample *t*-test was used to assess the possibility of significant differences between the two groups. All analyses were conducted using the SPSS 13.0 package for Windows (SPSS Inc., Cary, NC, USA); $P<0.05$ was considered statistically significant.

Accession numbers of nucleotide sequences
The nucleotide sequences have been deposited in the GenBank under the accession numbers KF999673–KF999679 and KJ949142–KJ949150 for the ^{13}C-archaeal and bacterial *amoA* genes from the DNA-SIP experiment, respectively. The pyrosequencing reads of the *amoA* and 16S rRNA genes have been deposited in the DNA Data Bank of Japan under the accession number DRA002271 and DRA001268, respectively.

Results

Soil nitrification activity
Soil nitrification activity was assessed by measuring changes in the nitrate concentration during the incubation of microcosms in the absence of acetylene, a suicide inhibitor of autotrophic ammonia oxidation (Figure 2a). Urea fertilization led to the stepwise production of NO_3^--N in the absence of C_2H_2 over an incubation course of 56 days, and we observed no significant difference in the concentrations of inorganic nitrogen between the $^{13}CO_2$-labeled and $^{12}CO_2$ control microcosms at day 56 (Supplementary Figure S2). Assuming linear kinetics, the net nitrification activity was estimated as the rate of increase in the soil nitrate concentration, which showed a decreasing trend from ZY to JD to LZ and finally to JX, with ~11.9, 9.46, 3.03 and 1.43 μg NO_3^--N g^{-1} d.w.s. per day, respectively. This was further supported by an increasing trend in the soil ammonium concentrations, with ~119,

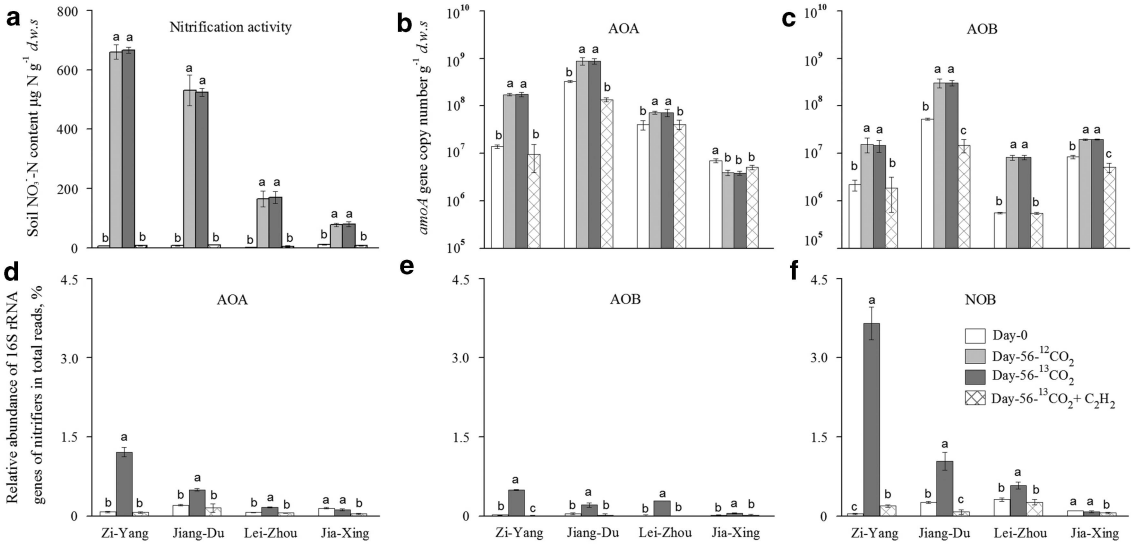

Figure 2 Change in nitrification activity and community structures of ammonia oxidizers and nitrite oxidizers in soil microcosms over an incubation period of 56 days. AOA, AOB and NOB represent ammonia-oxidizing archaea, bacteria and nitrite-oxidizing bacteria in total DNA extract from microcosms, respectively. Soil nitrate production (**a**) was analyzed to assess nitrification activity in soil microcosms incubated with $^{12}CO_2$, $^{13}CO_2$ or $^{13}CO_2 + C_2H_2$ for 56 days. The *amoA* gene copy numbers of AOA (**b**) and AOB (**c**) were determined using real-time quantitative PCR. Pyrosequencing was performed at the total microbial community level in SIP microcosms using the universal primer pair 515F–907R, and the relative abundance of AOA (**d**), AOB (**e**) and NOB (**f**) is expressed as the ratio of the targeted 16S rRNA gene reads to the total microbial 16S rRNA gene reads in each microcosm. Each soil microcosm received 100 μg urea-N g^{-1} d.w.s. on a weekly basis. Day 56 indicates a soil microcosm that had been incubated for 56 days. $^{13}CO_2 + C_2H_2$ represents soil microcosms incubated with $^{13}CO_2$ in the presence of the nitrification inhibitor acetylene (C_2H_2). The designations next to x axis represent the soil sampling sites of paddy fields as shown in Figure 1. All treatments were conducted in triplicate microcosms. The error bars represent the standard errors of the mean of the triplicate microcosms. The different letters above the columns indicate a significant difference ($P<0.05$) based on the analysis of variance.

243, 600 and 706 μg NH_4^+-N g^{-1} d.w.s. for the ZY, JD, LZ and JX soils, respectively (Supplementary Figure S2). The addition of C_2H_2 completely inhibited the production of nitrate in all soils tested over a 56-day incubation period. Pairwise comparisons between the soil microcosms amended with and without C_2H_2 indicated that the consumption of soil ammonium from urea hydrolysis was recovered in an almost stoichiometric amount based on the nitrate produced in all soils tested over the 56-day incubation course (Supplementary Figure S2).

Population size and composition of the soil-nitrifying communities

The population sizes of AOA and AOB were determined using quantitative PCR of the *amoA* genes in microcosms at days 0 and 56 (Figures 2b and c). In the absence of C_2H_2, the copy numbers of the archaeal *amoA* genes increased by 12.4-, 2.67- and 1.83-fold in the microcosms of the ZY, JD and LZ soils at day 56 following urea addition at day 0; specifically, the copy numbers increased from 1.4×10^7 to 1.7×10^8, 3.3×10^8 to 8.8×10^8, and 4.0×10^7 to 7.3×10^7 g^{-1} d.w.s., respectively (Figure 2b). However, the copy numbers declined from 7.0×10^6 to 5.1×10^6 in the JX soil. The bacterial *amoA* gene copies increased significantly from 2.2×10^6, 5.3×10^7, 5.5×10^5 and 8.4×10^6 g^{-1} d.w.s. at day 0 to 1.6×10^7, 3.0×10^8, 8.2×10^6 and 2.0×10^7 g^{-1} d.w.s. at day 56 in the ZY, JD, LZ and JX soils, representing 7.27-, 5.66-, 14.8- and 2.38-fold increases, respectively (Figure2c). The addition of C_2H_2 completely abolished the increase in *amoA* gene abundance in both the AOA and AOB populations in all four soils.

Pyrosequencing of the 16S rRNA genes was performed at the whole microbial community level in the SIP microcosms of the four soils after incubation for 0 and 56 days. Approximately 450 000 high-quality 16S rRNA reads were obtained, and targeted reads from putative AOA, AOB and NOB sequences were selected for subsequent analysis (Supplementary Table S2). The relative abundance of AOA was generally higher than that of AOB in all soils tested at day 0, whereas it appeared that the AOB population was stimulated to a greater extent than the AOA population after incubation for 56 days. The AOA relative abundance increased from 0.88‰, 1.60‰ and 0.69‰ at day 0 to 12.4‰, 5.05‰ and 1.64‰ in the ZY, JD and LZ soils at day 56, representing 14.0-, 3.15- and 2.38-fold increases, respectively (Figure 2d). A similar trend was observed for the AOB relative abundance, which was increased by 22.5-fold (ZY), 4.92-fold (JD) and 138-fold (LZ) after incubation of the microcosm for 56 days (Figure 2e). The NOB population was also strongly stimulated by 83.0-, 4.01- and 1.83-fold in the ZY, JD and LZ soils, respectively (Figure 2f). In the JX soil, however, both AOA and NOB showed

slight declines, although a 2.26-fold increase in AOB was observed after incubation for 56 days.

Pyrosequencing of the *amoA* genes in the total DNA extracts from ^{13}C-labeled microcosms at days 0 and 56 was performed. The total numbers of high-quality *amoA* reads were ~280 000 and 182 000 for AOA and AOB, respectively (Supplementary Table S2).The phylogeny of the *amoA* genes was largely congruent with that of the 16S rRNA genes for both AOA (Supplementary Figure S3) and AOB (Supplementary Figure S4). Most archaeal *amoA* reads were classified into the soil group 1.1b lineage, including nine distinct OTUs within four clusters: the soil fosmid 29i4 cluster, the 29i4-associated cluster, the soil fosmid 54d9 cluster and the *Nitrososphaera viennensis* cluster (Supplementary Figure S3a). Phylogenetic analysis of the archaeal 16S rRNA genes further revealed the presence of thermophilic AOA-like sequences, but no reads could be assigned to the soil fosmid 54d9 cluster (Supplementary Figure S3b). As for AOB, the phylogenetic analysis of both the *amoA* genes and the 16S rRNA genes indicated high sequence similarity to members within the *Nitrosomonas communis* cluster and the *Nitrosospira* clusters 0 and 3 (Supplementary Figure S4). The bacterial *amoA* genes were clustered into seven OTUs (Supplementary Figure S4a), which was consistent with the 16S rRNA gene analysis (Supplementary Figure S4b). With respect to NOB, all 16S rRNA gene sequences fell exclusively within the genus *Nitrospira* and *Nitrobacter* (Supplementary Figure S5). The *Nitrospira moscoviensis*-like OTU-1 dominated the nitrite oxidizer populations. The *Nitrospira defluvii* cluster was composed of three unique OTUs, whereas two OTUs were affiliated with the *Nitrospira marina* cluster. There was only one unique OTU-7 within the *Nitrobacter hamburgensis* cluster (Supplementary Figure S5).

SIP of active nitrifying communities

Isopycnic centrifugation of the total DNA extract was performed to resolve the ^{13}C-labeled DNA from the^{12}C native DNA in the four paddy soils after incubation for 56 days (Figure 1). Real-time quantitative PCR of the *amoA* genes in the fractionated DNA showed strong labeling of the AOA populations in the ZY and JD soils and strong labeling of the AOB populations in all four soils tested (Figure 3). In the microcosms of the SIP controls ($^{12}CO_2$ and$^{13}CO_2 + C_2H_2$), the highest *amoA* copy numbers of both AOA and AOB were detected in the 'light' fractions typical for the unlabeled DNA, with a buoyant density of ~1.720 g ml^{-1}. However, in the $^{13}CO_2$-labeled microcosms, archaeal *amoA* genes in the ZY and JD soils peaked in 'heavy' DNA fractions, with buoyant densities of ~1.740 g ml^{-1}, suggesting that the genome of the AOA populations was labeled and spun down during the isopycnic ultracentrifugation of the total DNA extract (Figures 3a and c). In the $^{13}CO_2$-labeled microcosms of the LZ soil, a small amount of archaeal *amoA* gene copies was detected in the 'heavy' fraction (Figure 3e), whereas no apparent peak of archaeal *amoA* genes was observed in the JX soil (Figure 3g). By contrast, most bacterial *amoA* genes could be retrieved in the 'heavy' DNA fractions of all four soils tested. The highest copy number of bacterial *amoA* genes was observed in the 'heavy' fractions, with buoyant densities of 1.730–1.735 g ml^{-1} for the ZY and JD soils (Figures 3b and d), whereas the peaks occurred in the heavier fractions of 1.740 g ml^{-1} for the LZ and JX soils (Figures 3f and h). Labeling of *amoA* genes was not observed in the SIP microcosms amended with $^{13}CO_2 + C_2H_2$, suggesting that $^{13}CO_2$ assimilation by AOA and AOB was dependent on ammonia oxidation in this study (Figure 3). The pyrosequencing of 16S rRNA genes at the whole microbial community level further revealed significant enrichments of AOA, AOB and NOB, accounting for up to 30.0%, 36.0% and 58.1% of the total microbial communities in the 'heavy' DNA fractions, respectively (Supplementary Table S3). This was not observed in the SIP control microcosms (Supplementary Table S3), suggesting chemolithoautotrophic lifestyles of active nitrifiers tested (Supplementary Results).

Clone libraries were constructed from the ^{13}C-*amoA* genes for phylogenetic analysis (Figure 4a). The 29i4 clusters contained 95%, 60% and 80% of the ^{13}C-labeled archaeal *amoA* clones in the ZY, JD and LZ soils, respectively (Table 2). Approximately 20% of the labeled archaeal *amoA* genes in the JD soil fell into the 29i4-associated cluster. In addition, 5%, 20% and 20% of the labeled archaeal *amoA* genes in the ZY, JD and LZ soils, respectively, could be assigned to the *N. viennensis* cluster (Table 2). Similar results were obtained for the^{13}C-labeled 16S rRNA genes (Figure 4b). Archaeal communities were predominated by members within the 29i4 cluster, accounting for 94.3%, 71.6% and 64.0% of the ^{13}C-labeled 16S rRNA genes in the ZY, JD and LZ soils, respectively. Furthermore, 21.8% and 36.0% of the labeled 16S rRNA genes showed a high sequence similarity with AOA within the *N. viennensis* cluster in the JD and LZ soils, respectively (Table 2).

As for active AOB (Supplementary Figure S6a), 95%, 50%, 100% and 50% of the ^{13}C-labeled bacterial *amoA* genes were phylogenetically closely related to *Nitrosospira* cluster 3 in the ZY, JD, LZ and JX soils, respectively (Table 2). *Nitrosomonas communis*-like AOB comprised 50% of the ^{13}C-labeled *amoA* genes in the JD soil, whereas 50% of the ^{13}C-labeled bacterial *amoA* genes were affiliated with *Nitrosospira* cluster 0 in the JX soil. Similar results were observed for the ^{13}C-labeled 16S rRNA genes (Supplementary Figure S6b). For instance, ~91.4%, 38.2%, 100% and 55.4% of the ^{13}C–16S rRNA genes could be assigned to *Nitrosospira* cluster 3 in the ZY, JD, LZ and JX soils,

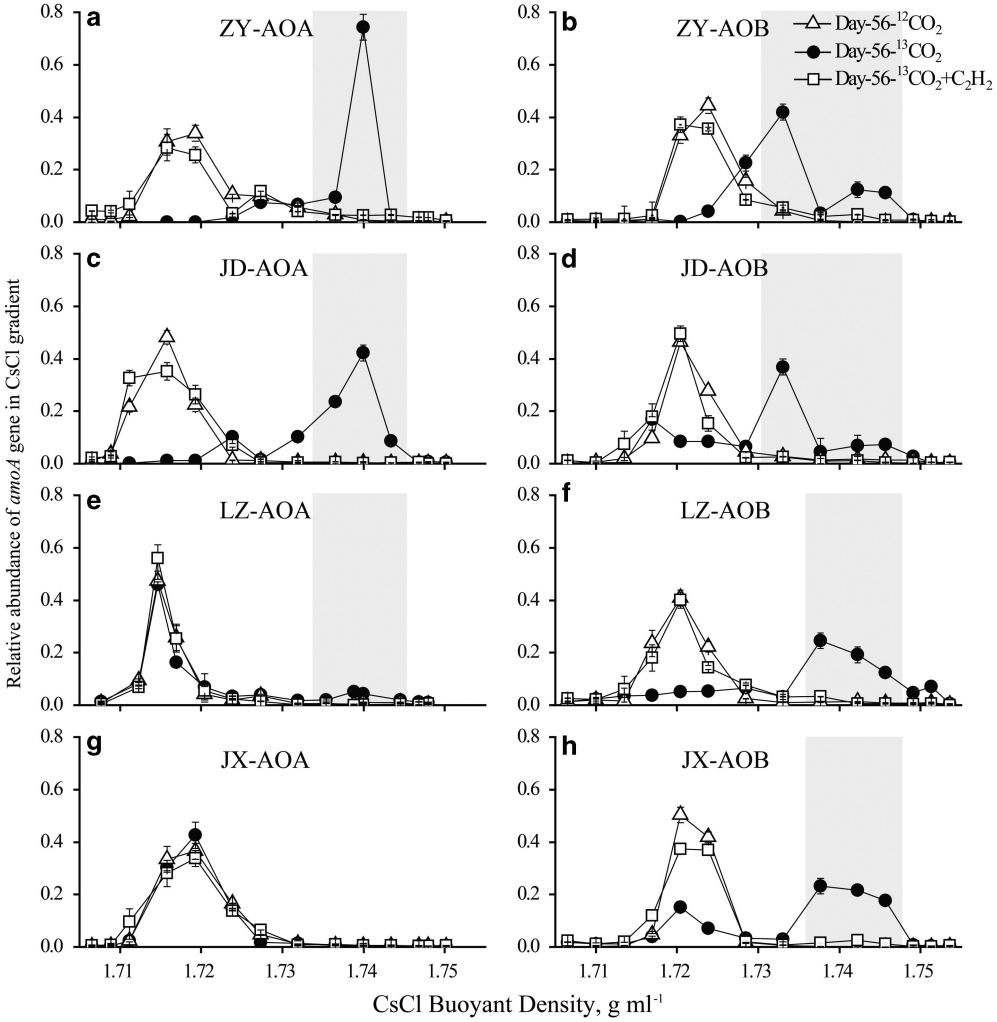

Figure 3 The quantitative distribution of the archaeal and bacterial *amoA* genes across the entire buoyant density gradient of the DNA fractions from soil microcosms incubated with $^{12}CO_2$, $^{13}CO_2$ or $^{13}CO_2 + C_2H_2$ for 56 days. The normalized data are the ratios of the gene copy number in each DNA fraction to the sum of the *amoA* genes across the entire gradient of DNA fractions for each treatment. The shaded area indicates the active fractions (^{13}C labeled) from the labeled microcosms. The active fraction for ^{13}C-AOA showed a narrow range of buoyant density from 1.735 to 1.745 mg l^{-1} for soils of ZY, JD and LZ. The ^{13}C-AOB were observed in active fractions with DNA buoyant density from 1.730 to 1.745 mg l^{-1} for ZY and JD, and from 1.735 to 1.745 mg l^{-1} for LZ and JX soils, respectively. The error bars represent the standard errors of the triplicate microcosms, and each contains three technical replications. All other designations are the same as those in Figures 1 and 2.

respectively (Table 2). Meanwhile, the *Nitrosomonas communis* cluster comprised 61.8% of the ^{13}C-labeled AOB in the JD soil, whereas 43.6% of active AOB were grouped into *Nitrosospira* cluster 0 in the JX soil. The ^{13}C-labeled 16S rRNA genes of nitrite oxidizers were affiliated with known NOB (Supplementary Figure S7) and were predominated by *Nitrospira*- rather than *Nitrobacter*-like NOB (Table 2).

Correlating soil properties with ammonia oxidizers and nitrite oxidizers

The potential relationship between ammonia oxidize and soil properties under *in situ* conditions (day 0) were inferred through unconstrained (BIO-ENV) (Clarke and Ainsworth, 1993) and constrained (CCA) multivariate analysis. The paddy soils were slightly acidic to moderately alkaline, ranging from a pH of 6.08 in the JX soil to a pH of 8.28 in the ZY soil (Table 1). The OXC increased from ZY (7.40 mmol kg^{-1}) to JD (9.21 mmol kg^{-1}) to LZ (19.9 mmol kg^{-1}) and finally to JX (27.3 mol kg^{-1}). The LZ and JX soils contained much lower SOM than the ZY and JD soils. Furthermore, a 2-month flooding of the paddy soil in the laboratory indicated that the cumulative soil oxygen concentration in ZY (19.2 μg l^{-1}) and JD (20.5 μg l^{-1}) soils were significantly lower than that of LZ (128 μg l^{-1}) and JX (183 μg l^{-1}) soils (Figure 5a).

The BIO-ENV analysis showed the best correlations of OXC, pH, NO_3^-, SOM and TN to the ammonia oxidizer population under *in situ*

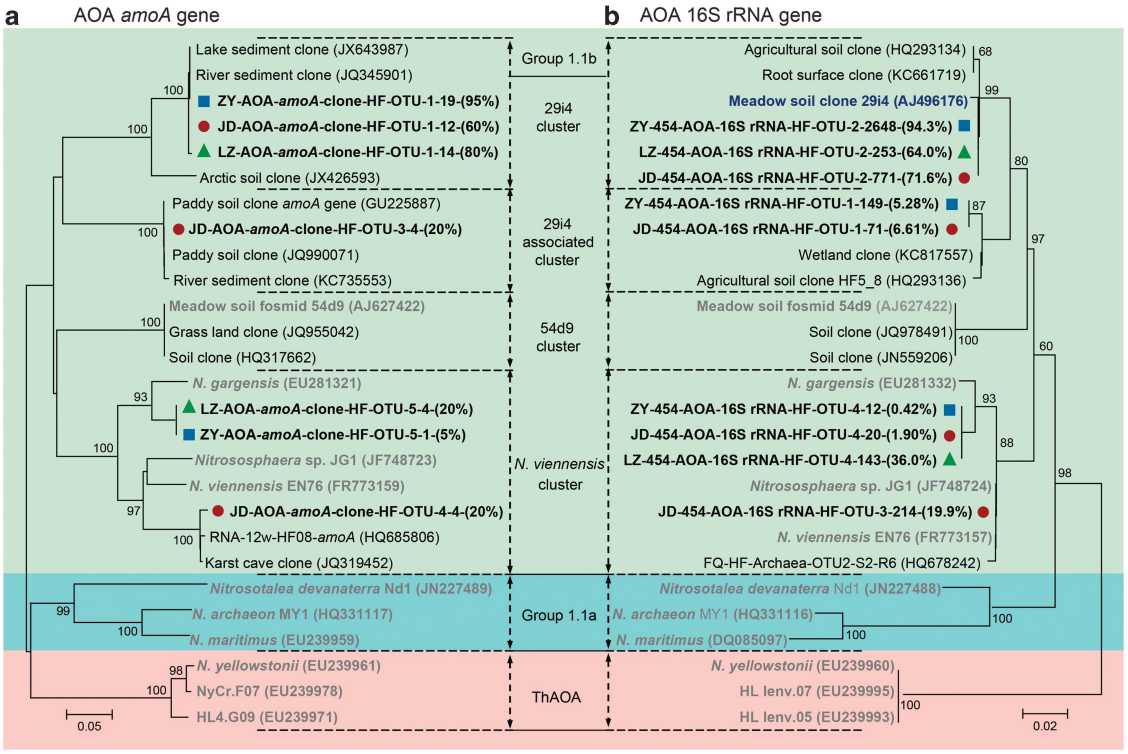

Figure 4 Phylogenetic analysis of the *amoA* (**a**) and 16S rRNA genes (**b**) of AOA in ^{13}C-labeled DNA from the $^{13}CO_2$-treated microcosms after an incubation period of 56 days. The designation 'HF' indicates the ^{13}C-DNA in the active fraction after the ultracentrifugation of the total DNA extract from the labeled microcosm. The designation 'ZY-454-AOA-16S rRNA-HF-OTU-1-149-(5.28%)' indicates that OTU-1 contains 149 reads with >97% sequence similarity, accounting for 5.28% of the total archaeal AOA 16S rRNA gene reads in the ^{13}C-DNA from the ZY soil microcosms. Data normalization for each OTU was performed by the random extraction of 5000 reads of the 16S rRNA gene for analysis. One representative sequence from each OTU was selected using the mothur software for tree construction. Sequences obtained from different paddy soils are indicated by color symbols for ZY (■), JD (●) and LZ (▲). The sequences from organisms for which both 16S rRNA and *amoA* gene sequences are known were shown in gray. ZY-rRNA-OTU-1 indeed showed high sequence similarity to the enrichment culture of the fosmid 29i4 lineage (highlighted in blue), of which the *amoA* counterpart is still missing (Alves *et al*., 2013). Bootstrap values higher than 50% are indicated at branch nodes. The scale bars represent 2% and 5% nucleic acid sequence divergence for the 16S rRNA and *amoA* genes, respectively. All other designations are the same as those in Figures 1 and 2.

conditions based on *amoA* gene phylogeny (Supplementary Table S5). CCA analysis also showed that the combination of these soil properties explained the highest percentage of variance (Figure 5b). The first CCA axis was represented by TN ($r=-0.86$, $P<0.05$) and NO_3^- ($r=-0.85$, $P<0.01$) and could explain 47.2% of the variance in the ammonia oxidizer phylotypes under *in situ* conditions. The second CCA axis was indicative of OXC ($r=0.95$, $P<0.01$), pH ($r=-0.66$, $P<0.05$) and SOM ($r=-0.72$, $P<0.01$), and it explained 37.6% of this variance. The active ammonia oxidizers were closely related to the pH, OM and OXC along with CCA axis 2 (Figure 5b). For instance, the ^{13}C-labeled OTUs 1, 3 and 4 of the AOA populations were associated with a slightly alkaline soil pH, SOM and a low soil OXC. In contrast, the ^{13}C-labeled AOB phylotypes of OTU-2 and OTU-5 showed a close relationship with a low soil pH and SOM in addition to a high soil OXC, whereas OTU-7 was closely related to a high SOM (Supplementary Table S6).

Discussion

More than 50% of the world's population feeds on rice, most of which is cultivated under waterlogged conditions and intensive fertilization regimes. This imposes dual selection pressures on nitrifying populations, as oxygen and ammonia serve as the major energy-generating compounds for ammonia and nitrite oxidizers. Our results provide compelling evidence for the functional importance of AOA, AOB and NOB during active nitrification in paddy soil. Archaeal contributions decreased from ZY to JD to LZ, whereas the AOB were solely responsible for ammonia oxidation in the JX soil. Statistic analysis further indicated a significant relationship of the ^{13}C-AOA/AOB ratio to OXC.

DNA-SIP relies entirely on cell proliferation, and $^{13}CO_2$ assimilation by AOA and AOB cells depends solely on the energy generated from ammonia oxidation (Figure 3). The AOA/AOB ratio in ^{13}C-DNA could thus largely represent the relative importance of AOA and AOB during active soil

Table 2 Proportions of active nitrifying populations in the density-resolved ^{13}C-DNA from the SIP microcosms of soils from different geographic regions

Nitrifier	*Phylotype*[a]	*^{13}C-amoA genes*				*^{13}C-16S rRNA genes*			
		Zi-Yang (%)	*Jiang-Du (%)*	*Lei-Zhou (%)*	*Jia-Xing (%)*	*Zi-Yang (%)*	*Jiang-Du (%)*	*Lei-Zhou (%)*	*Jia-Xing (%)*
AOA	Soil 29i4 fosmid	95	60	80	—	94.3	71.6	64.0	—
	29i4 associated	—	20	—	—	5.28	6.61	—	—
	Nitrososphaera viennensis	5.0	20	20	—	0.42	21.8	36.0	—
AOB	*Nitrosospira* cluster 3	95	50	100	50	91.4	38.2	100	55.4
	Nitrosospira cluster 0	—	—	—	50	—	—	—	43.6
	Nitrosomonas communis	5.0	50	—	—	8.59	61.8	—	1.01
NOB	*Nitrospiramos coviensis*	NA	NA	NA	NA	52.6	15.2	7.31	31.8
	Nitrospira defluvii	NA	NA	NA	NA	38.0	69.0	88.8	26.0
	Nitrospira marina	NA	NA	NA	NA	6.86	4.02	3.89	37.6
	Nitrobacter hamburgensis	NA	NA	NA	NA	2.54	11.8	—	4.62

Abbreviations: AOA, ammonia-oxidizing archaea; AOB, ammonia-oxidizing bacteria; NA, not applicable for NOB; NOB, nitrite-oxidizing bacteria; SIP, stable-isotope probing.
The dashed line indicates that no sequences were detected.
[a]Phylogenetic affiliations of active nitrifiers are delineated in Figure 4 (AOA), Supplementary Figure S6 (AOB) and Supplementary Figure S7 (NOB).

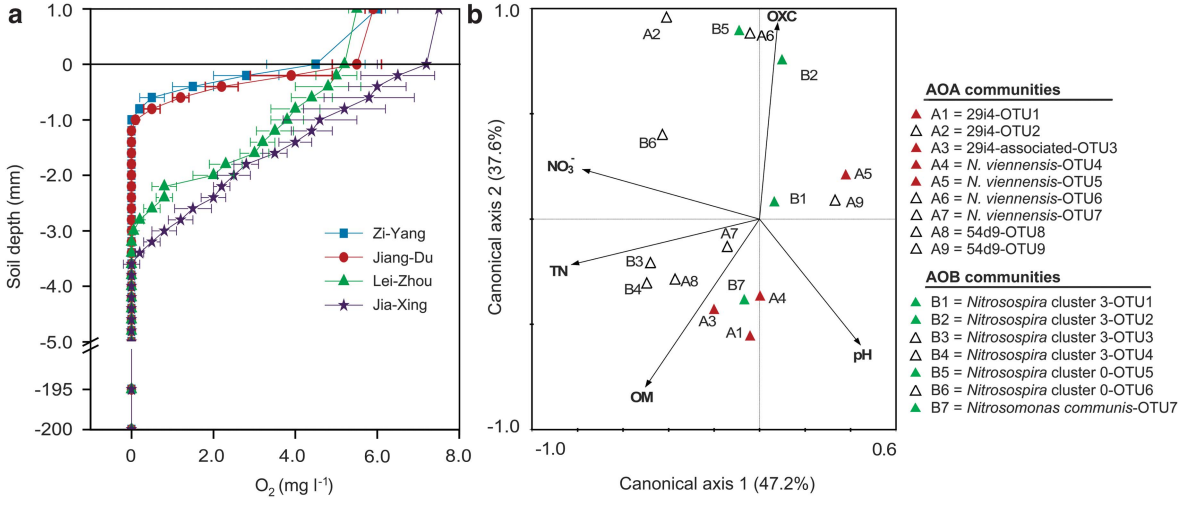

Figure 5 Vertical profiles of the oxygen concentrations of the flooding rice soils (**a**) and canonical correlation biplot analysis (**b**) between ammonia oxidizers and physiochemical characteristics of the four paddy soils in field. Soil oxygen concentration was measured using a Unisense oxygen microelectrode (±s.e., $n=3$). The phylotypes of ammonia oxidizers were grouped on the basis of *amoA* gene sequences, and the percentages of phylotype distribution variance that can be explained by the two principal canonical axes are shown within the parentheses near the axes. The phylotype proportion (PR) of ammonia oxidizers was normalized on the basis of the population size of AOA and AOB in soil microcosms using the equation $PR = r \times A/(A+B)$, where A and B denote the population sizes of AOA and AOB, respectively, based on the *amoA* gene copy numbers in soil (d.w.s.), and where 'r' denotes the relative abundance of a phylotype in the AOA or AOB populations as revealed by the pyrosequencing of *amoA* genes. The designations A1–A9 refer to the AOA phylotypes, whereas B1–B7 denote the AOB phylotypes as shown in Supplementary Figure S9. Active AOA and AOB in the ^{13}C-DNA are indicated by red and green triangles, respectively. Conditional variables are represented by black arrows. The abbreviations OM, OXC and TN represent the soil organic matter, oxidation capacity and total nitrogen, respectively. All other designations are the same as those in Figure 2.

nitrification. The quantitative analysis of *amoA* genes revealed that the AOA/AOB ratios in the ^{13}C-labeled DNA were37.0, 10.5 and 1.91 in ZY, JD and LZ soils, respectively, whereas AOB were exclusively detected in the JX soil (Supplementary Table S4).This was further supported by pyrosequencing the^{13}C-DNA of the total microbial communities (Supplementary Table S3), which showed similar patterns of AOA/AOB 16S rRNA gene ratios of 6.25, 1.40 and 0.12 in the soils of ZY, JD and LZ, respectively. These results indicated important roles for archaeal ammonia oxidation in

ZY soil. In fact, assuming the soil nitrate generation resulted solely from bacterial ammonia oxidation, the observed nitrate production of the ZY soil would have necessitated a cell-specific rate of AOB of up to 131.1 fmol N per cell h^{-1}(Supplementary Table S4), which far exceeds the highest rate identified thus far in any known ammonia oxidizer (Koops *et al.*, 2006). Nonetheless, the labeling of AOA and AOB depends on $^{13}CO_2$ assimilation in this study, and the relationship between CO_2 fixation and ammonia oxidation is poorly understood. The recent study has shown that AOA possess the most energy-efficient pathway for CO_2 fixation (Könneke *et al.*, 2014), suggesting the mole ratio of NH_3 oxidation to C incorporation differ greatly among AOA and AOB species (Belser, 1984; Feliatra and Bianchi, 1993). It is also noteworthy that the uptake efficiency of carbon and nitrogen by AOA from urea hydrolysis remained unclear (Alonso-Sáez *et al.*, 2012; Lu and Jia, 2013), although the putative archaeal *ureC* genes were detected in this study (Supplementary Figure S8).

The results of this study showed the predominant role of AOA in a slightly alkaline soil. Global examination has suggested the widespread presence and high abundance of AOA members within soil group 1.1b in non-acidic soil (Bates *et al.*, 2011). Meta-analyses of archaeal *amoA* genes at global, regional and local scales strongly suggested better adaption of this AOA group to relatively higher pH values (Gubry-Rangin *et al.*, 2011; Hu *et al.*, 2013), but its function has remained elusive in complex soil environments (Schleper and Nicol, 2010). Our results indicated the greatest labeling of AOA in the ZY soil with a pH value as high as 8.23, suggesting the apparent outcompetition of AOA over AOB. The ZY soil in this study had an ammonia concentration of 368 μM under *in situ* conditions. Fertilizing soils on a weekly basis might have further enhanced soil ammonia contents throughout the incubation period (Supplementary Figure S2), indicating a broader substrate specificity of AOA than previously thought (Verhamme *et al.*, 2011). In addition, it is noteworthy that active AOA fell well within a newly proposed 29i4 lineage, a representative culture of which was recently isolated from arctic soil at a low temperature (Alves *et al.*, 2013). Rapid growth of AOA occurred at 28 °C in the ZY and JD soils, which were largely similar to the field conditions at the time of the soil sampling. This suggests that the low temperatures of arctic regions may not be the only factor that determines the structure and activity of this uncharacterized AOA lineage. Tundra fen soil was indeed found under flooding conditions, and statistical analysis suggested that soil moisture has important roles in the selection of this AOA group in arctic soil (Alves *et al.*, 2013).

In waterlogged rice systems, soil OXC could largely represent redox potential and might have important roles in shaping the structure of AOA and AOB. Flooding led to the rapid depletion of oxygen and generated distinct vertical profiles of oxygen concentrations in the four soils (Figure 5a). The sequential reduction of alternative electron acceptors occurred after oxygen depletion (Thauer *et al.*, 1977). The ZY and JD soils showed much lower values of OXC (Table 1) and lower oxygen concentrations than the LZ and JX soils. In addition, SOM is often considered a reducing agent (Liesack *et al.*, 2000) and could be significantly enhanced under long-term flooding management (Kalbitz *et al.*, 2013). Interestingly, SOM was almost two times higher in the ZY and JD soils than in the LZ and JX soils (Table 1), which was consistent with the soil OXC and oxygen patterns. Combined, these results suggest that the active AOA members within the 29i4 lineage might be better adapted to microaerophilic environments under relatively reducing conditions. For example, the highest labeling of AOA was observed in ZY soil that was flooded during the fallow seasons (Supplementary Table S3), making it similar to the waterlogged conditions of tundra fens in the field (Alves *et al.*, 2013). Genomic analysis has suggested that the ammonia oxidation pathway of AOA may be distinct from that of AOB, requiring only 0.5 O_2 per molecule of NH_3 oxidized (Walker *et al.*, 2010). Batch culture studies indeed demonstrated an extraordinarily high affinity for oxygen in AOA isolates from marine (Martens-Habbena *et al.*, 2009) and soil environments (Kim *et al.*, 2012). This was further substantiated by the recent findings that AOA are more tolerant to low-oxygen conditions than AOB in pure cultures (French *et al.*, 2012) and field investigations (Pett-Ridge *et al.*, 2013).

Without prior knowledge of the microorganisms actively involved in nitrite oxidation, high-throughput pyrosequencing of the total 16S rRNA genes in the ^{13}C-DNA provided an almost unbiased profiling strategy for identification of active NOB at an unprecedented level of coverage (Supplementary Table S3). NOB were labeled to a much greater extent than AOA and AOB (Supplementary Table S3). This could be explained by the higher growth rate and faster generation turnover of NOB than ammonia oxidizers under substrate-rich conditions (Morrill and Dawson, 1962), leading to greater ^{13}C incorporation into NOB genomes. However, phylogenetically distinct NOB species in the paddy soil were labeled to different extents, suggesting that they have different contributions to nitrite oxidation (Table 2). *Nitrospira*-like sequences were exclusively detected in the LZ soil and were overwhelmingly predominant in the NOB populations in the ^{13}C-labeled DNA of the four paddy soils tested in this study (Table 2). In contrast, the highest relative abundance of *Nitrobacter*-like sequences accounted for only up to11.8% of the active NOB populations in the JD paddy soil, which was significantly lower than the 41.0% in a upland alkaline soil (Xia *et al.*, 2011). This implied a stronger competitive

advantage of *Nitrospira*-like over *Nitrobacter*-like NOB in the paddy soils than in the upland soil, which might be attributed to better adaption of the former to the low concentrations of nitrite and oxygen compared with the latter (Schramm *et al.*, 1999, 2000; Lücker *et al.*, 2010). For instance, *Nitrospira moscoviensis* showed optimal growth at a low-nitrite concentration of 0.35 mmol l^{-1}(Ehrich *et al.*, 1995), and the complete inhibition of a novel marine *Nitrospira*-like bacteria was observed with nitrite concentrations of only 1.5 mmol l^{-1}(Off *et al.*, 2010). Furthermore, it is also likely that the majority of *Nitrobacter* grew on organic carbon (Daims *et al.*, 2001), and cannot be labeled with $^{13}CO_2$ in this study (Table 2). This may explain the apparently low diversity of active *Nitrobacter*-like NOB (Supplementary Figure S4). The cultivation of environmentally representative NOB would help to better understand the functional kinetics and population ecology of nitrite oxidizers in complex soil.

The results of this study might largely reflect the functional process of nitrification under field conditions, although the incubation of SIP microcosms could not entirely reproduce the physiochemical and biological characteristics of the paddy soils *in situ*. For instance, the ^{13}C-AOA, AOB and NOB at day 56 remained largely similar to those at day 0 (Supplementary Figure S9). Statistic analysis showed that the total microbial communities were clearly separated on the basis of the four sampling sites rather than the two time-points of days 0 and 56 (Supplementary Figure S10), implying there was no significant changes of microbial community structures during incubation of SIP microcosms. Furthermore, the surface soil used in this study was subjected to plowing every year after rice harvesting and was exposed to regular flooding and drainage management. This agricultural management very likely reduced the soil heterogeneity of the paddy field, implying that active nitrifying populations in this study could to some extent represent nitrification naturally occurring in rice field.

Taken together, the results of this study provide strong evidence for the differential contributions of AOA, AOB and NOB on the nitrification activities of four paddy soils. DNA-SIP clearly indicated that AOA within soil group 1.1b dominated ammonia oxidation in a slightly alkaline ZY paddy soil, whereas active ammonia oxidizers in neutral JX soil were exclusively associated with the AOB populations. Nitrite oxidation was predominantly catalyzed by phylogenetically distinct phylotypes of the *Nitrospira*-like rather than the *Nitrobacter*-like NOB. Our results suggest that the anthropogenic wetlands of paddy fields are likely to have selected for distinct nitrifying communities, and the tight interactions between ammonia oxidizers and nitrite oxidizers might be closely related to the physiochemical properties of soil, including its pH and redox conditions.

Conflict of Interest

The authors declare no conflict of interest.

Acknowledgements

We are grateful to Drs Shengnan Li and Jianjun Wang at the Institute of Geography and Limnology of the Chinese Academy of Sciences (CAS) for determination of soil oxygen profile. We thank Profs Renkou Xu, Guoliang Ji, Jinling Yang, Biao Huang and Jiuyu Li at the Institute of Soil Science for suggestions on the soil physiochemical characteristics, Mr Yu Shi for statistical analysis, Ms Rong Huang for pyrosequencing of *amoA* genes and our lab colleagues for helpful discussions. The three anonymous reviewers are gratefully acknowledged for constructive comments. This work was supported by the National Science Foundation of China (41090281 and 41101227), the Strategic Priority Research Program of the CAS (XDB15040000) and the Distinguished Young Scholar Program of the Jiangsu Province (BK2012048).

References

Alonso-Sáez L, Waller AS, Mende DR, Bakker K, Farnelid H, Yager PL *et al.* (2012). Role for urea in nitrification by polar marine Archaea. *Proc Natl Acad Sci USA* **109**: 17989–17994.

Alves RJE, Wanek W, Zappe A, Richter A, Svenning MM, Schleper C *et al.* (2013). Nitrification rates in Arctic soils are associated with functionally distinct populations of ammonia-oxidizing archaea. *ISME J* **7**: 1620–1631.

Bannert A, Mueller-Niggemann C, Kleineidam K, Wissing L, Cao ZH, Schwark L *et al.* (2011). Comparison of lipid biomarker and gene abundance characterizing the archaeal ammonia-oxidizing community in flooded soils. *Biol Fertil Soils* **47**: 839–843.

Bates ST, Berg-Lyons D, Caporaso JG, Walters WA, Knight R, Fierer N. (2011). Examining the global distribution of dominant archaeal populations in soil. *ISME J* **5**: 908–917.

Belser LW. (1984). Bicarbonate uptake by nitrifiers: effects of growth rate, pH, substrate concentration, and metabolic inhibitors. *Appl Environ Microbiol* **48**: 1100–1104.

Berg P, Klemedtsson L, Rosswall T. (1982). Inhibitory effect of low partial pressures of acetylene on nitrification. *Soil Biol Biochem* **14**: 301–303.

Bock E, Wagner M. (2006). Oxidation of inorganic nitrogen compounds as an energy source. In: Dwokin M, Falkow S (eds) *The Prokaryotes*. Springer: New York, NY, YSA, pp 457–495.

Chen XP, Zhu YG, Xia Y, Shen JP, He JZ. (2008). Ammonia-oxidizing archaea: important players in paddy rhizosphere soil? *Environ Microbiol* **10**: 1978–1987.

Clarke KR, Ainsworth M. (1993). A method of linking multivariate community structure to environmental variables. *Mar Ecol Prog Ser* **92**: 205–219.

Daims H, Nielsen JL, Nielsen PH, Schleifer K-H, Wagner M. (2001). *In situ* characterization of *Nitrospira*-like nitrite-oxidizing bacteria active in wastewater treatment plants. *Appl Environ Microbiol* **67**: 5273–5284.

Dam B, Dam S, Kim Y, Liesack W. (2014). Ammonium induces differential expression of methane and nitrogen metabolism-related genes in *Methylocystis* sp. strain SC2. *Environ Microbiol;* e-pub ahead of print 18 February 2014; doi:10.1111/1462-2920.12367.

Ehrich S, Behrens D, Lebedeva E, Ludwig W, Bock E. (1995). A new obligately chemolithoautotrophic, nitrite-oxidizing bacterium, *Nitrospira moscoviensis* sp. nov. and its phylogenetic relationship. *Arch Microbiol* **164**: 16–23.

Feliatra F, Bianchi M. (1993). Rates of nitrification and carbon uptake in the Rhone River plume (northwestern Mediterranean Sea). *Microb Ecol* **26**: 21–28.

Food and Agricultural Organization of the United Nations (FAO) (2014). Statistics Division of the Food and Agricultural Organization of the United Nations (FAOSTAT). FAO. Available at: http://faostat3.fao.org/faostat-gateway/go/to/download/R/RF/E (last accessed 18 August 2014).

Francis CA, Roberts KJ, Beman JM, Santoro AE, Oakley BB. (2005). Ubiquity and diversity of ammonia-oxidizing archaea in water columns and sediments of the ocean. *Proc Natl Acad Sci USA* **102**: 14683–14688.

Freitag TE, Chang L, Prosser JI. (2006). Changes in the community structure and activity of betaproteobacterial ammonia-oxidizing sediment bacteria along a freshwater-marine gradient. *Environ Microbiol* **8**: 684–696.

French E, Kozlowski JA, Mukherjee M, Bullerjahn G, Bollmann A. (2012). Ecophysiological characterization of ammonia-oxidizing archaea and bacteria from freshwater. *Appl Environ Microbiol* **78**: 5773–5780.

Galloway JN, Townsend AR, Erisman JW, Bekunda M, Cai Z, Freney JR *et al.* (2008). Transformation of the nitrogen cycle: recent trends, questions, and potential solutions. *Science* **320**: 889–892.

Gruber N, Galloway JN. (2008). An Earth-system perspective of the global nitrogen cycle. *Nature* **451**: 293–296.

Gubry-Rangin C, Hai B, Quince C, Engel M, Thomson BC, James P *et al.* (2011). Niche specialization of terrestrial archaeal ammonia oxidizers. *Proc Natl Acad Sci USA* **108**: 21206–21211.

Herrmann M, Saunders AM, Schramm A. (2009). Effect of lake trophic status and rooted macrophytes on community composition and abundance of ammonia-oxidizing prokaryotes in freshwater sediments. *Appl Environ Microbiol* **75**: 3127–3136.

Hu HW, Zhang LM, Dai Y, Di HJ, He JZ. (2013). pH-dependent distribution of soil ammonia oxidizers across a large geographical scale as revealed by high-throughput pyrosequencing. *J Soils Sediments* **13**: 1439–1449.

Hyman M, Arp D. (1992). $^{14}C_2H_2$- and $^{14}CO_2$-labeling studies of the de novo synthesis of polypeptides by *Nitrosomonas europaea* during recovery from acetylene and light inactivation of ammonia monooxygenase. *J Biol Chem* **267**: 1534–1545.

Jia ZJ, Conrad R. (2009). Bacteria rather than Archaea dominate microbial ammonia oxidation in an agricultural soil. *Environ Microbiol* **11**: 1658–1671.

Kalbitz K, Kaiser K, Fiedler S, Kölbl A, Amelung W, Bräuer T *et al.* (2013). The carbon count of 2000 years of rice cultivation. *Global Change Biol* **19**: 1107–1113.

Ke XB, Angel R, Lu YH, Conrad R. (2013). Niche differentiation of ammonia oxidizers and nitrite oxidizers in rice paddy soil. *Environ Microbiol* **15**: 2275–2292.

Kim JG, Jung MY, Park SJ, Rijpstra WIC, Sinninghe Damsté JS, Madsen EL *et al.* (2012). Cultivation of a highly enriched ammonia-oxidizing archaeon of thaumarchaeotal group I.1b from an agricultural soil. *Environ Microbiol* **14**: 1528–1543.

Kimura M. (2000). Anaerobic microbiology in waterlogged rice fields. In: Bollag JM, Stotzky G (ed) *Soil Biochemistry*. Marcel Dekker: New York, NY, USA, pp 35–138.

Klotz MG, Stein LY. (2008). Nitrifier genomics and evolution of the nitrogen cycle. *FEMS Microbiol Lett* **278**: 146–156.

Koops HP, Purkhold U, Pommerening-Roser A, Timmermann G, Wagner M. (2006). The lithoautotrophic ammonia-oxidizing bacteria. In: *The Prokaryotes*. Springer: New York, NY, USA, pp 778–811.

Könneke M, Bernhard AE, de la Torre JR, Walker CB, Waterbury JB, Stahl DA. (2005). Isolation of an autotrophic ammonia-oxidizing marine archaeon. *Nature* **437**: 543–546.

Könneke M, Schubert DM, Brown PC, Hügler M, Standfest S, Schwander T *et al.* (2014). Ammonia-oxidizing archaea use the most energy-efficient aerobic pathway for CO_2 fixation. *Proc Natl Acad Sci USA* **111**: 8239–8244.

Lehtovirta-Morley LE, Stoecker K, Vilcinskas A, Prosser JI, Nicol GW. (2011). Cultivation of an obligate acidophilic ammonia oxidizer from a nitrifying acid soil. *Proc Natl Acad Sci USA* **108**: 15892–15897.

Liesack W, Schnell S, Revsbech NP. (2000). Microbiology of flooded rice paddies. *FEMS Microbiol Rev* **24**: 625–645.

Liew EF, Tong D, Coleman NV, Holmes AJ. (2014). Mutagenesis of the hydrocarbon monooxygenase indicates a metal centre in subunit-C, and not subunit-B, is essential for copper-containing membrane monooxygenase activity. *Microbiology* **160**: 1267–1277.

Lu L, Jia ZJ. (2013). Urease gene-containing Archaea dominate autotrophic ammonia oxidation in two acid soils. *Environ Microbiol* **15**: 1795–1809.

Lücker S, Wagner M, Maixner F, Pelletier E, Koch H, Vacherie B *et al.* (2010). A *Nitrospira metagenome* illuminates the physiology and evolution of globally important nitrite-oxidizing bacteria. *Proc Natl Acad Sci USA* **107**: 13479–13484.

Martens-Habbena W, Berube PM, Urakawa H, de la Torre JR, Stahl DA. (2009). Ammonia oxidation kinetics determine niche separation of nitrifying Archaea and Bacteria. *Nature* **461**: 976–979.

Morrill LG, Dawson JE. (1962). Growth rates of nitrifying chemoautotrophs in soil. *J Bacteriol* **83**: 205–206.

Off S, Alawi M, Spieck E. (2010). Enrichment and physiological characterization of a novel *Nitrospira*-like bacterium obtained from a marine sponge. *Appl Environ Microbiol* **76**: 4640–4646.

Pett-Ridge J, Petersen DG, Nuccio E, Firestone MK. (2013). Influence of oxic/anoxic fluctuations on ammonia oxidizers and nitrification potential in a wet tropical soil. *FEMS Microbiol Ecol* **85**: 179–194.

Prosser JI, Nicol GW. (2012). Archaeal and bacterial ammonia-oxidisers in soil: the quest for niche specialisation and differentiation. *Trends Microbiol* **20**: 523–531.

Rotthauwe J, Witzel K, Liesack W. (1997). The ammonia monooxygenase structural gene *amoA* as a functional marker: molecular fine-scale analysis of natural

ammonia-oxidizing populations. *Appl Environ Microbiol* **63**: 4704–4712.
Santoro AE, Buchwald C, McIlvin MR, Casciotti KL. (2011). Isotopic signature of N_2O produced by marine ammonia-oxidizing archaea. *Science* **333**: 1282–1285.
Schleper C, Nicol GW. (2010). Ammonia-oxidising archaea—physiology, ecology and evolution. In: Robert KP (eds) *Advances in Microbial Physiology*. Academic PressNew York, NY, USA, pp 1–41.
Schloss PD, Westcott SL, Ryabin T, Hall JR, Hartmann M, Hollister EB *et al.* (2009). Introducing mothur: open-source, platform-independent, community-supported software for describing and comparing microbial communities. *Appl Environ Microbiol* **75**: 7537–7541.
Schramm A, de Beer D, Gieseke A, Amann R. (2000). Microenvironments and distribution of nitrifying bacteria in a membrane-bound biofilm. *Environ Microbiol* **2**: 680–686.
Schramm A, de Beer D, van den Heuvel JC, Ottengraf S, Amann R. (1999). Microscale distribution of populations and activities of *Nitrosospira* and *Nitrospira* spp. along a macroscale gradient in a nitrifying bioreactor: quantification by *in situ* hybridization and the use of microsensors. *Appl Environ Microbiol* **65**: 3690–3696.
Sebilo M, Mayer B, Nicolardot B, Pinay G, Mariotti A. (2013). Long-term fate of nitrate fertilizer in agricultural soils. *Proc Natl Acad Sci USA* **110**: 18185–18189.
Sorokin DY, Lucker S, Vejmelkova D, Kostrikina NA, Kleerebezem R, Rijpstra WIC *et al.* (2012). Nitrification expanded: discovery, physiology and genomics of a nitrite-oxidizing bacterium from the phylum *Chloroflexi*. *ISME J* **6**: 2245–2256.
Stieglmeier M, Mooshammer M, Kitzler B, Wanek W, Zechmeister-Boltenstern S, Richter A *et al.* (2014). Aerobic nitrous oxide production through *N*-nitrosating hybrid formation in ammonia-oxidizing archaea. *ISME J* **8**: 1135–1146.
Tamura K, Dudley J, Nei M, Kumar S. (2007). MEGA4: Molecular Evolutionary Genetics Analysis (MEGA) software version 4.0. *Mol Biol Evol* **24**: 1596–1599.
Thauer RK, Jungermann K, Decker K. (1977). Energy conservation in chemotrophic anaerobic bacteria. *Microbiol Mol Biol Rev* **41**: 100–180.
Tourna M, Freitag TE, Nicol GW, Prosser JI. (2008). Growth, activity and temperature responses of ammonia-oxidizing archaea and bacteria in soil microcosms. *Environ Microbiol* **10**: 1357–1364.
Verhamme DT, Prosser JI, Nicol GW. (2011). Ammonia concentration determines differential growth of ammonia-oxidising archaea and bacteria in soil microcosms. *ISME J* **5**: 1067–1071.
Walker CB, de la Torre JR, Klotz MG, Urakawa H, Pinel N, Arp DJ *et al.* (2010). *Nitrosopumilus maritimus* genome reveals unique mechanisms for nitrification and autotrophy in globally distributed marine crenarchaea. *Proc Natl Acad Sci USA* **107**: 8818–8823.
Webster G, Embley TM, Freitag TE, Smith Z, Prosser JI. (2005). Links between ammonia oxidizer species composition, functional diversity and nitrification kinetics in grassland soils. *Environ Microbiol* **7**: 676–684.
Xia WW, Zhang CX, Zeng XW, Feng YZ, Weng JH, Lin XG *et al.* (2011). Autotrophic growth of nitrifying community in an agricultural soil. *ISME J* **5**: 1226–1236.
Yan X, Akimoto H, Ohara T. (2003). Estimation of nitrous oxide, nitric oxide and ammonia emissions from croplands in East, Southeast and South Asia. *Glob Change Biol* **9**: 1080–1096.
Zhang JB, Cai ZC, Cheng Y, Zhu TB. (2009). Denitrification and total nitrogen gas production from forest soils of Eastern China. *Soil Biol Biochem* **41**: 2551–2557.

Supplementary Information accompanies this paper on The ISME Journal website (http://www.nature.com/ismej)